ELSEVIER

Solid State Ionics 98 (1997) 7–13

SOLID STATE IONICS

Oxygen permeation of $La_{0.3}Sr_{0.7}CoO_{3-\delta}$

C.H. Chen[1], H.J.M. Bouwmeester*, R.H.E. van Doorn, H. Kruidhof, A.J. Burggraaf

Laboratory for Inorganic Materials Science, Faculty of Chemical Technology, University of Twente, P.O. Box 217, 7500 AE Enschede, The Netherlands

Received 8 July 1996; accepted 10 February 1997

Abstract

The oxygen permeability of dense $La_{0.3}Sr_{0.7}CoO_{3-\delta}$ membranes has been measured in the range 750–1100°C under various oxygen partial pressure gradients. A sweep gas method was employed. Results indicate that in the range of thickness 0.057–0.215 cm used in the present study, the oxygen flux is predominantly controlled by bulk diffusion across the membrane. The measured activation energy is 60 kJ mol^{-1}. By fitting the permeation data for various thicknesses to the transport equation obtained upon assuming linear kinetics for the surface exchange reactions and bulk ionic transport, we could derive the oxygen ionic conductivity and the characteristic membrane thickness. The latter quantity determines the transition from predominant control by diffusion to that by surface exchange. The ionic conductivity is about 0.5 S cm^{-1} at 1000°C. The characteristic thickness is extrapolated at a value of about 80 μm.

Keywords: Oxygen permeation; Perovskite oxide; Membrane

1. Introduction

Dense ceramic oxides exhibiting high oxide ion and electronic conductivity are of great interest for potential applications in oxygen separation and novel catalytic reactors [1]. In recent years, oxygen permeation studies of many mixed-conducting oxides have been reported. Amongst them perovskite oxides $(La,Sr)(Co,Fe)O_{3-\delta}$ have received particular attention. Teraoka and coworkers [2–4] were the first to report high oxygen fluxes through the cobalt-rich compositions. Although the ionic transference number for selected compositions in this series remains below a value of 0.01, the ionic conductivity may be 1–2 orders of magnitude higher than that of stabilized zirconia.

An obvious consideration to the design of the aforementioned applications is the functional dependence of the oxygen flux on membrane thickness and oxygen partial pressure difference across the membrane. Attention has already been drawn to the contribution of the surface exchange kinetics to the overall permeation rate [5]. A characteristic membrane thickness L_c has been defined, at which point the oxygen flux is under mixed control of the surface exchange kinetics and bulk diffusion. No significant gain in the oxygen flux can be realized by making membranes thinner than about $0.1L_c$. In the present study, the oxygen permeation through

*Corresponding author.

[1]Present address: Laboratory for Applied Inorganic Chemistry, Delft University of Technology, Julianalaan 136, 2628 BL Delft, The Netherlands.

PII S0167-2738(97)00097-0

$La_{0.3}Sr_{0.7}CoO_{3-\delta}$ is investigated under various experimental conditions. The data obtained are used to calculate the oxygen ionic conductivity of the material and its characteristic membrane thickness.

2. Theory

2.1. Wagner equation

The rate at which oxygen permeates through a non-porous ceramic membrane is essentially controlled by two factors: the rate of oxygen diffusion across the membrane and that of interfacial oxygen exchange. When the flux is governed by bulk oxygen diffusion it is generally described by Wagner's equation [6],

$$j_{O_2} = -\frac{RT}{4^2F^2L}\int_{\ln P'_{O_2}}^{\ln P''_{O_2}} t_{el}\sigma_{ion}\, d\ln P_{O_2}. \quad (1)$$

Here δ_{ion} is the ionic conductivity, t_{el} the electronic transference number, L the membrane thickness, while P'_{O_2} and P''_{O_2} are the oxygen partial pressures at the high and low pressure side of the membrane, respectively. Other parameters have their usual significance. For mixed conductors in which the electronic conduction predominates, i.e. $t_{el}\approx 1$, integration extends only over σ_{ion}. Differentiating Eq. (1) with respect to the lower integration limit yields,

$$\left(\frac{\partial j_{O_2}}{\partial \ln P'_{O_2}}\right)_{P''_{O_2}} = \sigma_{ion}\times\frac{RT}{4^2F^2L}. \quad (2)$$

Hence, the ionic conductivity at a given pressure of P'_{O_2} can be obtained experimentally from the slope of j_{O_2} versus $\ln P'_{O_2}$ at that P'_{O_2}, provided that P''_{O_2} is kept constant during the experiment. Similarly, σ_{ion} can be evaluated from permeation data measured by varying P''_{O_2}, keeping P'_{O_2} at a fixed value.

2.2. Mixed controlled kinetics

In the case where the oxygen flux is also partly governed by the surface exchange reactions, the total chemical potential difference drop $\Delta\mu^{total}_{O_2}$ $(=RT\ln P''_{O_2}/P'_{O_2})$ is distributed across the membrane such that the rate determining process receives the greater proportion. For thick membranes bulk diffusion dominates, but as the thickness decreases the limited transfer across the interfaces becomes rate determining. Assuming linear kinetics for both bulk diffusion and surface exchange, the oxygen flux can be written as [1,5]

$$j_{O_2} = -\frac{1}{1+(2L_c/L)}\frac{\overline{t_{el}\sigma_{ion}}}{4^2F^2}\frac{\Delta\mu^{total}_{O_2}}{L}, \quad (3)$$

where $\overline{t_{el}\sigma_{ion}}$ is the mean value of the product over the applied oxygen pressure interval, and L_c the characteristic membrane thickness, defined by [7]

$$L_c = \frac{RT}{4^2F^2}\times\frac{\overline{t_{el}\sigma_{ion}}}{j^0_{ex}}. \quad (4)$$

Here the quantity j^0_{ex} (mol O_2 cm^{-2} s^{-1}) denotes the balanced exchange rate at the gas–solid interface in the absence of oxygen potential gradients. Comparing Eq. (3) with the Wagner equation (Eq. (1)), we see that the diffusional flux of oxygen across the membrane is reduced by $(1+2L_c/L)^{-1}$, relative to that in the absence of transfer limitations across the interfaces. The factor 2 in this expression takes into account the fact that there are two interfaces with identical properties, representing the general case of a symmetrical membrane. The total driving force $\Delta\mu^{total}_{O_2}$ is equally used for bulk diffusion and for the surface exchange when the thickness of the membrane equals $2L_c$.

The influence of the membrane thickness on oxygen flux calculated from Eq. (3) is shown in Fig. 1. When $L \gg L_c$, the oxygen flux varies inversely with L^{γ} where $\gamma=1$, which is in agreement with Wagner's theory. Departures from this inverse relationship are observed when the flux is partly governed by the surface exchange kinetics. The value of γ, at a given L, corresponds with the negative slope in the double logarithmic plot of the oxygen flux versus membrane thickness at that L. Taking the logarithm of Eq. (3), partial differentiation with respect to $\log L$ shows that γ is equal to the reduction factor $(1+2L_c/L)^{-1}$, the value of which gradually decreases with decreasing thickness to become zero for $L \ll L_c$, as is shown in Fig. 1. The

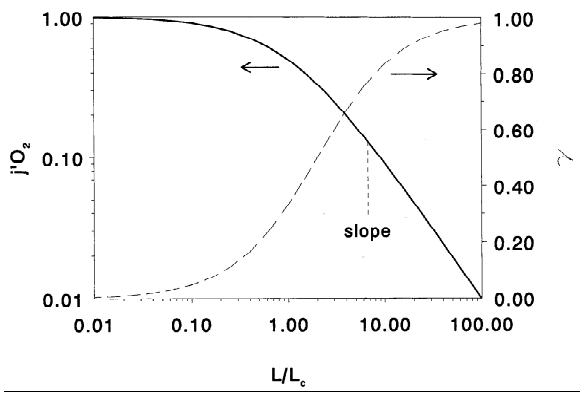

Fig. 1. Thickness dependence of the dimensionless oxygen flux j'_{O_2} calculated from Eq. (3). The quantity j'_{O_2} is defined by the ratio of the oxygen flux over the maximum achievable oxygen flux ($\frac{1}{2} j^0_{ex} \cdot \Delta\mu^{total}_{O_2}$) in the surface exchange limited regime. Only if $L \gg L_c$, the oxygen flux becomes proportional to $1/L^\gamma$ with $\gamma = 1$ in agreement with the Wagner theory. For smaller thicknesses, γ ranges between 1 and 0 (right hand scale).

latter situation corresponds with the maximum achievable flux, which for a symmetrical membrane is given by $\frac{1}{2} j^0_{ex} \Delta\mu^{total}_{O_2}$. It should be noted that, due to the linearised kinetics for bulk diffusion and surface exchange in its derivation, Eq. (3) neglects changes in material parameters with oxygen partial pressure. Without the knowledge thereof it should strictly be used only if small P_{O_2}-gradients appear across the membrane. In the general case, L_c will be a function of process parameters P_{O_2} and temperature.

3. Experimental

Powders of $La_{0.3}Sr_{0.7}CoO_{3-\delta}$ were prepared by adapting the aqueous sol–gel route originally proposed by Bilger et al. [8] for the preparation of $La_{0.8}6Sr_{0.14}MnO_3$. Details of the synthesis are described elsewhere [9]. Chemical analysis of the powder obtained after calcining at 800°C showed a slight cobalt excess. The real composition was $La_{0.32}Sr_{0.68}Co_{1.05}O_{3-\delta}$. X-ray powder diffraction indicated a single cubic perovskite phase. No evidence was found for any contamination or phase inhomogeneity. Powders were isostatically pressed at 400 MPa for 5 min into pellets (∅ = 1.6 cm), which were sintered at 1100°C for 10 h. The relative density was about 92%. These pellets were shaped into disks (∅ = 1.2 cm) and polished with 1000 MESH SiC to final thicknesses 0.215, 0.115, and 0.057 cm.

Oxygen permeation measurements were performed in the temperature range of 750–1100°C. Supremax glass rings (Schott, Nederland B.V.) were used to seal the disc specimen into the quartz permeation reactor at 1050°C. Prior to sealing, the side wall of the disc was covered with a paste based on fine Duran glass powder (Schott, Nederland B.V.) to avoid radial contributions to the oxygen flux. Oxygen/nitrogen mixtures and helium were passed along opposite membrane sides. The oxygen partial pressures at the immediate surfaces were taken to be similar to those measured down-stream, assuming ideal gas mixing conditions to hold in the reactor volume. Unless stated otherwise, the partial pressure at the oxygen-rich side was similar to that in ambient air. The one at the lean side of the membrane was controlled by adjusting the helium flow rate. Gas flow rates were controlled by Brooks 5800 mass flow controllers. Gas leakage, if present, could be detected gas chromatographically by the presence of nitrogen in the helium stream, and was found normally to be below 1%. Both the permeation reactor and the apparatus have been described in detail elsewhere [10,11].

Oxygen fluxes were normalized on the surface area exposed to the helium permeate stream. Corrections were applied for that portion of the membrane surface covered by the glass seal ring. Table 1 lists correction factors G for these edge-effects, which were obtained from a numerical procedure to solve the steady-state diffusion equation on the basis of Fick's second law (with a constant diffusion coefficient) in cylindrical coordinates [11]. The oxygen flux was calculated from

$$j_{O_2} = \frac{1}{G} \cdot \frac{F c^{permeate}_{O_2}}{A} \quad (5)$$

Table 1
Sample dimensions and flux correction factors

Thickness (cm)	Radius at P'_{O_2} side (cm)	Radius at P''_{O_2} side (cm)	G (cm)
0.057	0.6	0.45	1.113
0.11	0.6	0.45	1.230
0.215	0.6	0.45	1.388

where F ($cm^3\ s^{-1}$ (STP)) is the flow rate at the outlet of the reactor, $c_{O_2}^{permeate}$ ($mol\ cm^{-3}$) the oxygen concentration in the effluent stream and A (cm^2) the geometric surface at the helium side of the membrane.

4. Results and discussion

4.1. Temperature dependence

Arrhenius plots of oxygen permeation through $La_{0.3}Sr_{0.7}CoO_{3-\delta}$ specimens of different thickness are given in Fig. 2. The oxygen partial pressure difference across the membrane was fixed during measurement. Values for the oxygen partial pressures at both sides of the membrane and the measured activation energy are given in Table 2. The close match between the activation energies obtained upon varying the membrane thickness suggests that permeation through the specimens is controlled by a common rate determining step. As described below, this turns out to be bulk diffusion across the membrane.

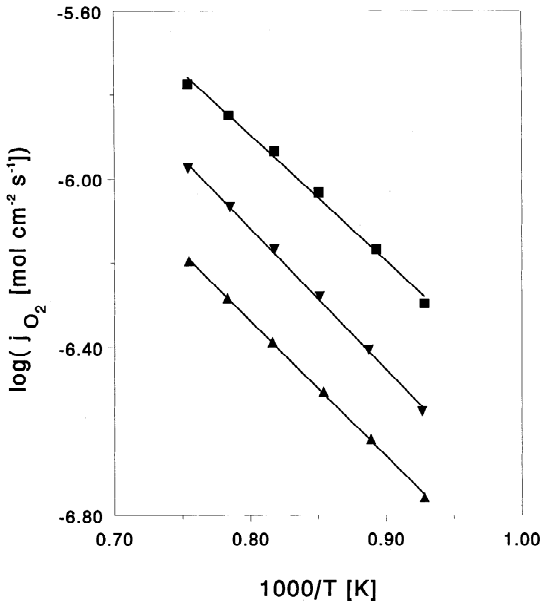

Fig. 2. Temperature dependence of the oxygen permeation rate of $La_{0.3}Sr_{0.7}CoO_{3-\delta}$. Thicknessses are (■) 0.057 cm, (▼) 0.115 cm and (▲) 0.215 cm. Experimental conditions are listed in Table 2.

Table 2
Experimental conditions and calculated activation energies

Thickness (cm)	P'_{O_2} (atm)	P''_{O_2} (atm)	E_{act} ($kJ\ mol^{-1}$)
0.057	0.21	0.033	64±1
0.115	0.21	0.023	57±2
0.215	0.21	0.016	62±7

4.2. Oxygen pressure dependence

Fig. 3 shows experimental permeation data at 1000°C as a function of oxygen partial pressure. During measurement the oxygen partial pressure at the opposite side of the membrane was kept at a fixed value. Under these experimental conditions, the oxygen flux varies almost linearly with the logarithm of oxygen partial pressure, even though some small divergence is seen for the thinnest specimen of 0.057 cm at the lowest oxygen partial pressures in Fig. 3b. In view of Eq. (2) a constant slope would indicate that the ionic conductivity remains invariant under changes in the oxygen partial pressure. Average values of the ionic conductivity of $La_{0.3}Sr_{0.7}CoO_{3-\delta}$ evaluated from the slopes of the curves in Fig. 3a and b are listed in Table 3.

The above observations agree well with existing data of oxygen non-stoichiometry of $La_{0.3}Sr_{0.7}CoO_{3-\delta}$ obtained from a thermogravimetric study performed by Mizusaki et al. [12], assuming the vacancy diffusion coefficient in the range of oxygen pressure to adopt a constant value. The authors showed that the nonstoichiometry, at 800°C and oxygen partial pressures similar to those used in the present study, varies approximately with $P_{O_2}^{-1/16}$. The absolute power was found to decrease even further with increasing temperature. With the additional assumption that all oxygen vacancies contribute to transport one would thus predict the ionic conductivity of $La_{0.3}Sr_{0.7}CoO_{3-\delta}$ to be almost invariant with P_{O_2}. Yet, a disagreement is apparent from Table 3 between σ_{ion} evaluated from j_{O_2} versus $\ln P'_{O_2}$ (Fig. 3a) and that from j_{O_2} versus $\ln P''_{O_2}$ (Fig. 3b). Since the analysis in terms of Eq. (2) is based upon ionic diffusion through the bulk as the rate limiting step in oxygen permeation, we attribute the observed discrepancy to partial rate control by the surface exchange reactions discussed below.

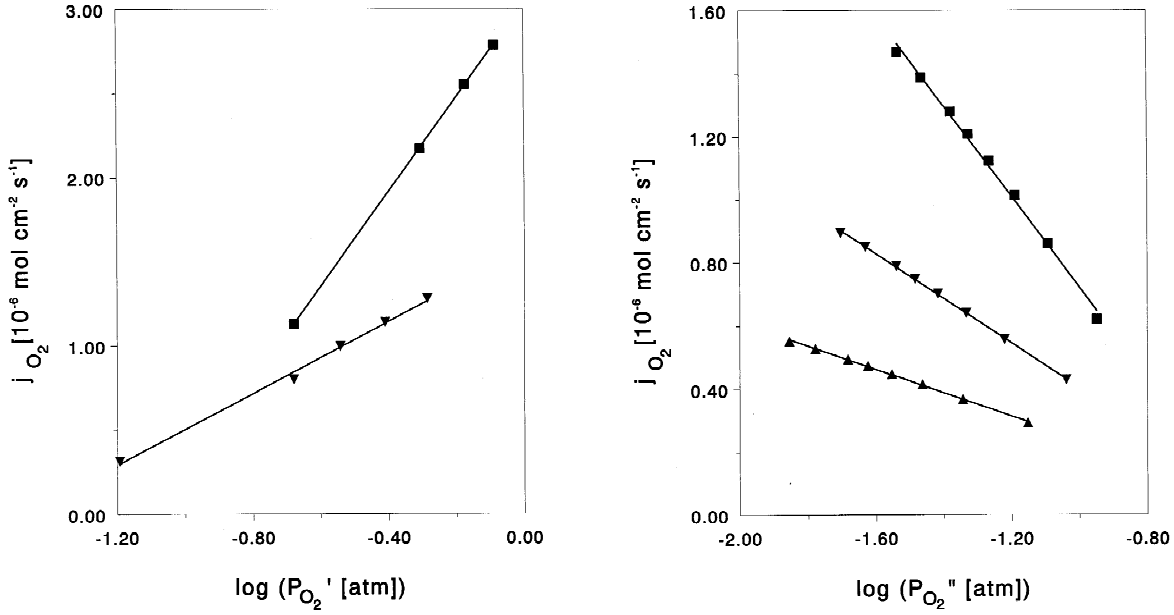

Fig. 3. Oxygen pressure dependence of the oxygen permeation rate of $La_{0.3}Sr_{0.7}CoO_{3-\delta}$ at 1000°C. (a) high-pressure side; (■) 0.057 cm, $P''_{O_2} = 0.053$ atm; (▼) 0.115 cm, $P'_{O_2} = 0.028$ atm. (b) low-pressure side; (■) 0.057 cm; (▼) 0.115 cm: (▲) 0.215 cm. Air ($P'_{O_2} = 0.21$ atm) is on the high-pressure side.

Table 3
Ionic conductivity of $La_{0.3}Sr_{0.7}CoO_{3-\delta}$ at 1000°C

Membrane thickness (cm)	σ_{ion} (S cm^{-1}) evaluated from j_{O_2} versus ln P'_{O_2} (Fig. 3a)	σ_{ion} (S cm^{-1}) evaluated from j_{O_2} versus ln P''_{O_2} (Fig. 3b)
0.057	0.98±0.05	0.50±0.01
0.115	0.75±0.03	0.50±0.01
0.215	–	0.49±0.01

4.3. Thickness dependence

A constant ionic conductivity of $La_{0.3}Sr_{0.7}CoO_{3-\delta}$, as a function of oxygen partial pressure as one would predict from data of oxygen non-stoichiometry, extends the applicability of Eq. (3) to investigate possible contributions of the surface exchange kinetics to the overall permeation rate. In Fig. 4, we show the log–log plot of the oxygen flux versus membrane thickness for three different temperatures 1000, 1050 and 1100°C, respectively, normalized to a value of P''_{O_2} of 0.05 atm. The oxygen flux is found to vary with $1/L^{\gamma}$ with $\gamma = 0.87 \pm 0.02$. Since γ is close to unity, this confirms that in the range of thicknesses and temperatures covered by the experiments bulk ionic diffusion determines the overall performance of the membrane. The deviation from the ideal inverse relationship between the oxygen flux and membrane thickness as predicted by Wagner's theory (Eq. (1)) is interpreted to reflect the partial rate limitation by the surface exchange kinetics.

Parameters obtained from fitting of Eq. (3) to the flux data are listed in Table 4, indicating that the characteristic thickness L_c at which point the transition from predominant control by bulk diffusion to that by surface exchange would occur at a thickness just below 100 μm. The latter value has also been quoted recently by Kilner [13] based upon analysis of data of isotopic exchange for a wide variety of

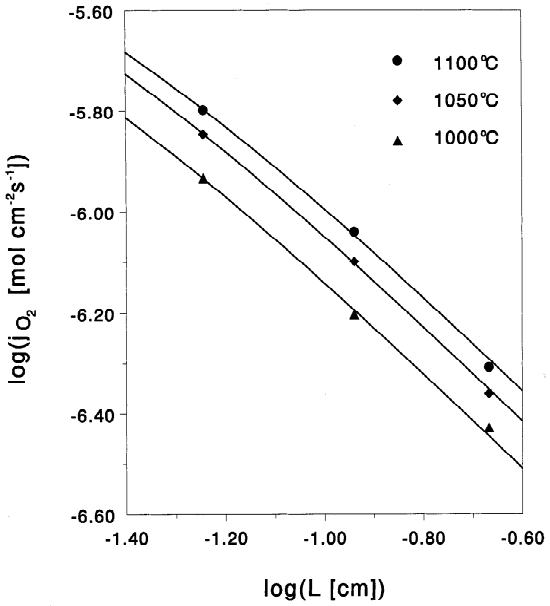

Fig. 4. Thickness dependence of the oxygen permeation rate of $La_{0.3}Sr_{0.7}CoO_{3-\delta}$. Data from Fig. 2, normalized to $P''_{O_2} = 0.05$ atm. Drawn lines indicate the fit to Eq. (3).

Table 4
Characteristic thicknesses L_c ionic conductivity σ_{ion} and surface exchange rate j_0^{ex} at different temperatures

Temperature (°C)	L_c (μm)	σ_{ion} (S cm^{-1})	j_0^{ex} (mol cm^{-2} s^{-1})
1000	68±20	0.81±0.04	$(8.4\pm3.7)\times10^{-6}$
1050	73±11	0.97±0.03	$(9.7\pm1.6)\times10^{-6}$
1100	87±21	1.08±0.06	$(9.5\pm2.3)\times10^{-6}$

mixed-conducting perovskites. As concerns the magnitude of the ionic conductivity, it may be noted that this favourably compares with the corresponding data given in Table 3.

The maximum obtainable flux is determined by the surface exchange rate. Values for j_{ex}^0 calculated from Eq. (4) are listed as well in Table 4. As noted before, no further advantage will be gained from making membranes thinner than O.1L_c. If extrapolation of the present data of values of P''_{O_2} of 10^{-4} atm is allowed, provided that such a low value of P''_{O_2} can be maintained under actual membrane operating conditions, it is easily calculated from Eq. (2) that the oxygen flux passing from the air side of a membrane of thickness of 10 μm can be as high as 3×10^{-5} mol O_2 cm^{-2} s^{-2} at 1000°C. An obvious consideration is that such a membrane needs to be supported by a porous substrate in order to provide sufficient mechanical integrity.

5. Conclusions

We have shown that the results from oxygen permeation measurements through dense $La_{0.3}Sr_{0.7}CoO_{3-\delta}$ membranes may be interpreted in terms of a simple model based upon linearised kinetics of bulk ionic transport and the surface exchange reactions. In the range of thickness 0.0577–0.215 cm used in the present study of bulk ionic transport mainly governs the overall rate of oxygen permeation. The ionic conductivity at 1000°C is estimated at about 0.5 S cm^{-1}. It is, however, evident that partial rate limitations occur by the surface exchange kinetics, since the permeation rate measured as a function of thickness departs from that expected for purely bulk-controlled kinetics. Calculations show that in the range of temperature 1000–1100°C the membranes operate under mixed control of the surface exchange kinetics and bulk diffusion at a characteristic thickness L_c estimated to be about 80 μm.

Acknowledgments

This study has been carried out in the framework of a collaboration programme between Academia Sinica and Dutch Academy of Sciences (KNAW) and has been financially supported by (KNAW). Prof Meng Guangyao (Department of Materials Science and Engineering, University of Science and Technology of China) is gratefully acknowledged for stimulating this project.

References

[1] H.J.M. Bouwmeester, A.J. Burggraaf, in: Fundamentals of Inorganic Membrane Science and Technology, A.J. Burggraaf and L. Cot (Eds.), Elseviers Science, Amsterdam, Ch. 10, pp. 435–528.

[2] Y. Teraoka, H.M. Zhang, S. Furukawa, N. Yalnazoe, Chem. Lett. (1985) 1743.
[3] Y. Teraoka, T. Nobunaga, N. Yamazoe, Chem. Lett. (1988) 503.
[4] Y. Teraoka, T. Nobunaga, K. Okamoto, N. Miura, N. Yamazoe, Solid State Ionics. 48 (1991) 207.
[5] H.J.M. Bouwmeester, H. Kruidhof, A.J. Burggraaf, Solid State Ionics. 72 (1994) 185.
[6] C. Wagner, Progr. Solid State Chem. 10(1) (1975) 3.
[7] Here we would like to note that a factor 2 is missing in Eq. (4) in Ref. 5. With the present definition of L_c, while using the Nernst–Einstein equation, it can be shown that $L_c = D^*/k_s$ when $t_{el} = 1$, where D^* is the tracer diffusion coefficient and k_s the surface exchange coefficient. Both parameters are accessible from ^{18}O–^{16}O isotopic techniques where the ratio D^*/k_s appears to be the fundamental parameter governing tracer diffusion bounded by a limiting surface exchange rate between lattice oxygen and oxygen from the ^{18}O-enriched gas phase.
[8] S. Bilger, E. Syskakis, A. Naoumidis, H. Nickel, J. Am. Ceram. Soc. 75 (1992) 964.
[9] C.H. Chen, H. Kruidhof, H.J.M. Bouwmeester, A.J. Burggraaf, Mater. Sci. and Eng. B. 39 (1996) 129.
[10] H.J.M. Bouwmeester, H. Kruidhof, A.J. Burggraaf, P.J. Gellings, Solid State Ionics. 53–56 (1992) 460.
[11] J.E. ten Elshof, H.J.M. Bouwmeester, H. Verweij, Solid State Ionics. 81 (1995) 97.
[12] J. Mizusaki, Y. Mima, S. Yamauchi, K. Fueki, J. Solid State Chem. 80 (1989) 102.
[13] J. Kilner, in: T.A. Ramanarayan, W.L. Worrell, H.L. Tuller (Eds.), Proc. 2nd Int. Symp. Ionic and Mixed Conducting Oxide Ceramics, The Electrochemical Society, Pennington, NJ, 1994, p. 174.